minerals

MDPI

Article

Degradation of Thiol Collectors Using Ozone at a Low Dosage: Kinetics, Mineralization, Ozone Utilization, and Changes of Biodegradability and Water Quality Parameters

Pingfeng Fu [1,2,*], Xiaofeng Lin [1], Gen Li [1], Zihao Chen [1] and Hua Peng [1]

[1] School of Civil and Resources Engineering, University of Science and Technology Beijing, Beijing 100083, China; lxf1120120338@163.com (X.L.); lone0622@163.com (G.L.); 18810969392@163.com (Z.C.); 13051510851@163.com (H.P.)

[2] Key Laboratory of High-Efficient Mining and Safety of Metal Mines, Ministry of Education, Beijing 100083, China

* Correspondence: pffu@ces.ustb.edu.cn; Tel.: +86-135-2020-2167

Received: 16 September 2018; Accepted: 19 October 2018; Published: 24 October 2018

Abstract: Ozonation at a high O_3 dosage can achieve high efficiencies in removing flotation reagents but it has a low ozone-utilization rate. The ozonation of potentially toxic thiol collectors (potassium ethyl xanthate (EX), sodium diethyl dithiocarbamate (SN-9), *O*-isopropyl-*N*-ethyl thionocarbamate (Z-200) and dianilino dithiophoshoric acid (DDA)) was investigated in an ozone-bubbled reactor at a low O_3 dosage of 1.125 mg/(min·L). The degradation kinetics, mineralization, ozone utilization, changes of biodegradability, and water quality parameters were studied, and the degradation behaviors of four collectors were compared. Thiol collectors could be effectively degraded with a removal ratio of >90% and a mineralization ratio of 10–27%, at a low O_3 dosage. The ozonation of thiol collectors followed the pseudo first-order kinetics, and rate constants had the order of $k_{\text{SN-9}} > k_{\text{EX}} > k_{\text{Z-200}} > k_{\text{DDA}}$. The Z-200 and DDA were the refractory flotation reagents treated in the ozonation process. After ozonation, the biodegradability of EX, SN-9, and DDA solutions was remarkably raised, but the biodegradability of Z-200 only increased from 0.088 to 0.15, indicating that the Z-200 and its intermediates were biologically persistent organics. After ozonation, the solution pH decreased from 10.0 to 8.0–9.0, and both the conductivity and oxidation-reduction potential increased. The ozone utilization ratio in decomposing thiol collectors was above 98.41%, revealing almost complete usage of input O_3. The results revealed that thiol collectors could be effectively degraded by O_3, even at a low dosage, but their degradation behaviors were quite different, due to intrinsic molecular properties.

Keywords: thiol collectors; flotation effluents; ozone; mineralization; biodegradability; ozone utilization; water quality parameters

---

1. Introduction

Froth flotation is extensively used to separate valuable minerals from sulfide ores. Thiol collectors, including xanthates, dithiophosphates, and dithiocarbamates, are important flotation reagents which can render sulfide minerals hydrophobic and facilitate bubble attachments [1]. As a huge amount of sulfide ores are treated annually by froth flotation, the quantities of consumed collectors are extremely large. Even in the 1980s, the global xanthate consumption per year was estimated to be more than 52,000 tons [2]. Therefore, thiol collectors and derived byproducts can be frequently encountered in flotation effluents. The hazards of xanthate to humans or aquatic lives have been comprehensively reviewed [3,4].

To reduce water consumption in mineral processing, the flotation effluents should be circulated into flotation circuits. However, in most cases, residual flotation reagents and their byproducts have negative effects on mineral flotation because these compounds can randomly alter the chemistry of flotation system [5,6]. Therefore, it is necessary to remove residual reagents from flotation effluents to improve water quality of flotation feeding water.

In the past decades, numerous methods have been developed to remove organic reagents from flotation effluents, such as coagulation and precipitation [7], adsorption [8], chemical oxidation [9], advanced oxidation [10–12], and biodegradation [13,14]. Adsorption is an efficient and simple technique in removing flotation reagents, but further treatment of sludge with toxic reagents and high water content becomes very difficult. The chemical oxidation with oxidants such as sodium hypochlorite often results in secondary pollution [9]. The biodegradation is a low-cost process for treating flotation effluents. However, the long treatment period [14] and the toxicity of some reagents to microbes [13,15] have limited its application in treating flotation effluents.

Recently, advanced oxidation processes (AOPs), involving ozone [10,11], Fenton's reagents [16], hydrogen peroxide [17], persulfate [18], photocatalysis [19], and photoelectrooxidation [20] have been studied to degrade organic flotation reagents, especially xanthates. As hydroxyl radicals (·OH) have an oxidation-reduction potential (ORP) of 2.8 V, the AOPs have exhibited high efficiency in decomposing flotation reagents and their intermediates. However, most of these reports have just been limited to the removal of xanthates [10,11,19,20], and little attention is paid to degrading the other thiol collectors, such as dithiophosphates and dithiocarbamates. Since the molecular structures of thiol collectors are quite different, their decomposition behaviors by the AOPs may be different from each other.

Among above mentioned AOPs, ozonation is one of the most promising processes in decomposing organic pollutants. Ozonation at a high O_3 dosage can effectively decompose xanthates with a remarkable reduction of COD and generation of SO_4^{2-} ions [10,11]. In the flotation of sulfide ores, the pulp pH is usually kept at 9–12 [21,22]. Thus, the alkalinity of flotation effluents can enhance the ozonation of organic reagents as OH^- ions are the catalyst in decomposing O_3 to generate·OH [23,24]. Additionally, from the viewpoints of practical applications, ozone can be generated in situ, using air or oxygen as sources, in mines, avoiding the transportation and storage of dangerous chemical oxidants such as H_2O_2 [17] and sodium hypochlorite [9]. Therefore, ozonation is considered to be an appropriate technique to treat flotation effluents in mines.

However, ozonation is somewhat disputed for high energy consumption in O_3 generation [25,26]. Thus the ozone utilization becomes very critical in economic valuation of ozonation. In our previous study, O_3 utilization in degrading *n*-butyl xanthate ranged from 7.2 to 51.7% at the O_3 dosage of 5.88–50.36 mg/(min·L) [11]. Even when ultraviolet radiation (UV) was combined to promote the decomposition of O_3, the O_3 utilization in UV/O_3 process only increased by 15–30%, compared to pure O_3 [11]. Liu et al. [10] observed fast degradation of butyl xanthate at high O_3 dosage of 145.59 mg/(min·L), but the O_3 utilization was not concerned. As the reagent concentration in flotation pulps is usually 10^{-3}–10^{-4} mol/L [27], the pollutant concentration in flotation effluents is much lower than that of pharmaceutical effluents and petrochemical wastewaters [28,29]. In ozonation, a lower concentration of organics usually leads to a declined O_3 decomposition rate, resulting in lower ozone utilization. Thus, a lower O_3 dosage might achieve a higher O_3 utilization, in the treatment of flotation effluents. Therefore, it is necessary to investigate the degradation efficiencies of flotation reagents and ozone utilization at low O_3 dosage.

In this study, four thiol collectors, potassium ethyl xanthate (EX), sodium diethyl dithiocarbamate (SN-9), *O*-isopropyl-*N*-ethyl thionocarbamate (Z-200), and dianilino dithiophoshoric acid (DDA), were selected as the sulfide mineral collectors. The O_3 dosage was controlled to be as low as 1.125 mg/(min·L), much lower than that previously used in the ozonation of xanthates [10,11]. The aims of this work were, (1) to investigate degradation kinetics, mineralization, and changes of biodegradability and water quality parameters in degrading thiol collectors using O_3, (2) to compare degradation efficiencies of thiol collectors with different molecular structures, and (3) to evaluate the ozone utilization and energy consumption efficiency at a low O_3 dosage. The result can provide fundamental aspects of ozone utilization and degradation behaviors of potentially toxic sulfide mineral collectors, at a low O_3 dosage.

2. Materials and Methods

2.1. Chemicals

The EX and SN-9 with analytical grade were purchased from Shanghai Aladdin Chemical Reagent Co., Ltd., Shanghai, China. The Z-200 and industrial grade DDA were purchased from Tieling Flotation Reagents Co. Ltd., China. Their molecular formulas, molecular structures, and abbreviations used are summarized in Table 1. By storing the collectors in a brown vacuum desiccator, they were separated from air and radiation, to prevent the oxidation. Other chemicals, such as iodine (I_2), potassium iodide (KI), silver sulfate (Ag_2SO_4), mercury sulfate ($HgSO_4$), and potassium bichromate ($K_2Cr_2O_7$) were of analytical grade and were purchased from Sinopharm Chemical Reagent Beijing Co., Ltd., Beijing, China. In all experiments, deionized water was used.

Table 1. Collector name, molecular formula, molecular structure, and abbreviations used in this work.

Collector Name	Molecular Formula	Molecular Structure	Abbreviation
potassium ethyl xanthate	$C_2H_4OCS_2K$	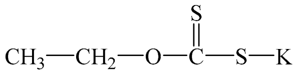 $CH_3-CH_2-O-\overset{\overset{S}{\|}}{C}-S-K$	EX
sodium diethyl dithiocarbamate	$(C_2H_5)_2NCSSNa$	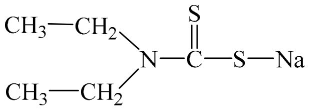 $(CH_3-CH_2)_2N-\overset{\overset{S}{\|}}{C}-S-Na$	SN-9
O-isopropyl-*N*-ethyl thionocarbamate	$(CH_3)_2CHOCSNHC_2H_5$	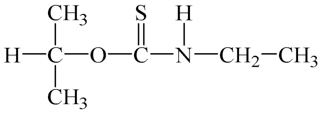 $H-\underset{CH_3}{\overset{CH_3}{C}}-O-\overset{\overset{S}{\|}}{C}-\overset{\overset{H}{\mid}}{N}-CH_2-CH_3$	Z-200
dianilino dithiophoshoric acid	$(C_6H_5NH)_2PSSH$	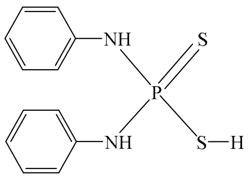	DDA

2.2. Experimental Procedures

All the degradation experiments were conducted with a batch mode in a jacket glass bubbled reactor connected to a thermostatic bath. The schematic diagram of experimental setup is shown in Figure 1. The cylindrical reactor, with a height of 1150 mm and internal diameter of 50 mm, was installed with a porous glass plate at the bottom to distribute the O_3 stream. Ozone was generated with air as the source, by an O_3 generator (SW-004, Qingdao West Electronic Purifiers Co., Qingdao, China). The O_3 stream was introduced into the reactor with a steady-state O_3 concentration of 1347 mg/m^3 and at a gas flow rate of 0.1 m^3/h. The degradation experiments were carried out at 25 ± 2 °C.

Prior to degradation experiments, the collector (0.2 g) was dissolved in 2 L deionized water to prepare an EX (SN-9, Z-200 or DDA) solution of 100 mg/L concentration. The initial pH was adjusted to 10.0 with 0.05 mol/L NaOH or HCl solution. While 2 L collector solution was introduced into the reactor, bubbled with an O_3 stream, the degradation began at the O_3 dosage of 1.125 mg/(min·L). As, the four different collectors had different degradation efficiencies, to achieve the collector removal ratio of 90–100%, for the comparison, the ozonation time was chosen to be 90, 90, 120, and 180 min for the EX, SN-9, Z-200, and DDA, respectively. The aqueous samples were taken at designed intervals to determine the concentrations of collector, SO_4^{2-} ions, COD, BOD_5, and TOC. The water quality parameters (pH, conductivity, oxidation-reduction potential (ORP)) were measured by immersing the electrodes into solutions as shown in Figure 1.

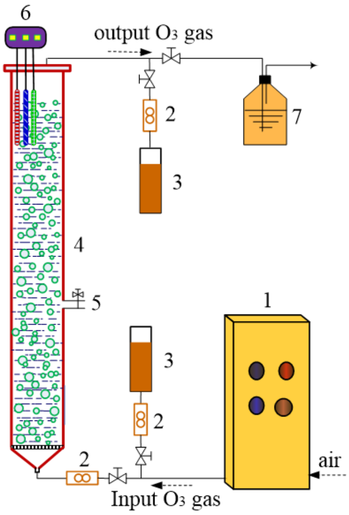

Figure 1. Schematic diagram of experimental setup. 1—ozone generator; 2—flow meter; 3—KI absorption liquid for measuring O_3 concentration; 4—bubbled cylindrical reactor; 5—sampling valve; 6—multi-parameter water quality meter (pH electrode, ORP electrode, conductivity probe); 7—ozone destructor bottle with KI solution.

2.3. Analysis and Calculation

2.3.1. Determination of the Collector Concentration

The xanthate concentration has always been determined by the UV-vis spectroscopic method. However, this method has seldom been reported to measure the concentration of the SN-9, Z-200 and DDA [13]. Figure 2a showed the UV-vis absorbance spectra of EX, SN-9, Z-200, and DDA solutions recorded by a UV-vis spectrophotometer (UV-5500PC, Shanghai Metash Instruments Co. Ltd., Shanghai, China). The maximum absorption peaks appeared at 301 nm for EX, 256 nm for SN-9, 241 nm for Z-200, and 230 nm for DDA solution, respectively. The plots of the collector concentration *versus* absorbance at its characteristic absorption wavelength are shown in Figure 2b. The correlation coefficients (>0.99) indicated that calibration curves could be used to calculate the collector concentration by recording its absorbance.

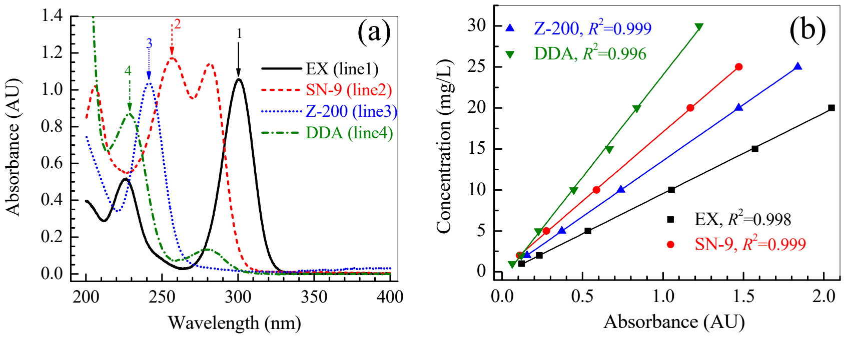

Figure 2. UV-vis absorbance spectra for the four collector solutions, at 20 mg/L concentration (**a**); and the collector concentration versus the absorbance of collector solutions (**b**).

Thus, in this work, the concentration of four collectors was determined by the UV-vis spectroscopic method. The removal ratio of the collector was calculated as the following:

$$\beta_{\text{collector}} = \frac{C_0 - C_t}{C_0} \times 100\% \quad (1)$$

where $\beta_{\text{collector}}$ was the removal ratio of the collector (EX, SN-9, Z-200 or DDA), C_0 and C_t (mg/L) were the collector concentration at initial and time t, respectively.

2.3.2. Determination of COD, BOD_5, TOC, and Concentration of ${SO_4}^{2-}$ ions

The chemical oxygen demand (COD) was determined by the standard dichromate method (HJ/T 399-2007). The biochemical oxygen demand (BOD_5) was detected by the classic dilution and inoculation method (HJ 505-2009). The aqueous samples were incubated at 20 °C, for 5 days. The total organic carbon (TOC) concentrations were measured using a Shimadzu TOC-V organic carbon analyzer. The concentration of ${SO_4}^{2-}$ ions was determined by a barium chromate spectrophotometry method (HJ/T 342–2007). In this study, the removal ratio of COD was obtained by Equation (2), as follows:

$$\beta_{\text{COD}} = \frac{COD_0 - COD_t}{COD_0} \times 100\% \quad (2)$$

where β_{COD} was the removal ratio of COD, COD_0 and COD_t (mg/L) were the COD concentration at initial and time t, respectively.

The carbon mineralization ratio was calculated by Equation (3), as follows:

$$\gamma_{\text{C}} = \frac{TOC_0 - TOC_t}{TOC_0} \times 100\% \quad (3)$$

where γ_{C} was the carbon mineralization ratio of the collector, and TOC_0 and TOC_t (mg/L) were the TOC concentration at initial and time t, respectively. As the ${SO_4}^{2-}$ ions, with the highest valence of sulfur, were the final products during the oxidation of organic sulfur in thiol collectors, the sulfur mineralization ratio was defined by Equation (4), as follows:

$$\gamma_{\text{S}} = \frac{M}{n \times 96} \times \frac{C_{\text{SO}_4^{2-},t}}{C_0} \times 100\% \quad (4)$$

where γ_{S} was the sulfur mineralization ratio of the collector, M and n were the molecular weight and number of sulfur atom in the collector molecule (EX, SN-9, Z-200 or DDA), respectively, $C_{\text{SO}_4^{2-},t}$ was the concentration of ${SO_4}^{2-}$ ions at time t, and C_0 (mg/L) was initial collector concentration.

2.3.3. Analysis of Water Quality Parameters

Water quality parameters of ozonated solutions, including solution pH, conductivity and ORP, were measured by a multi-parameter water quality meter equipped with different electrodes (Bante 900-UK, Shanghai Bante Instruments Co. Ltd., Shanghai, China). The solution pH was measured by a pH combination electrode (P11 mode). Before the measurement, it was calibrated with buffer solutions of pH 4.01, 7.00 and 10.01. The conductivity was determined by a glass conductivity probe with platinum cells (K10 mode). The ORP was recorded using an epoxy ORP electrode (501 mode), which was composed of a platinum pin and Ag/AgCl reference electrode.

2.3.4. Analysis of Gaseous O_3 Concentration

The gaseous O_3 concentration was determined by the KI absorption method (CJ/T 3028.2-94). The O_3 concentration in the output O_3 gas was measured after 30 min of ozonation to meet the solubility equilibrium of O_3 in solutions. The ozone utilization ratio was calculated by Equation (5), as follows:

$$\eta_{O3} = \frac{C_{O3,in} - C_{O3,out}}{C_{O3,in}} \times 100\% \tag{5}$$

where η_{O3} was the ozone utilization ratio, $C_{O3,in}$ and $C_{O3,out}$ (mg/m^3) were the O_3 concentration in input and output O_3 gas streams, respectively.

3. Results and Discussion

3.1. Degradation Kinetics of Thiol Collectors

The degradation behaviors of thiol collectors by O_3 are shown in Figure 3a. Figure 3b illustrated the logarithmic plot of $\ln(C_t/C_0)$ *versus* ozonation time t, and kinetic parameters were summarized in Table 2. As shown in Figure 3a, EX, and SN-9 were rapidly degraded by O_3, but the degradation of Z-200 and DDA were much slower. At 90 min, the removal ratio of EX and SN-9 was close to 100%, but only 87.38% of the Z-200 and 79.71% of the DDA were removed. By extending the ozonation time, 98.39% of Z-200 could be removed at 120 min, but only 90.91% of DDA was degraded even at 180 min. As shown in Figure 3b and Table 2, the removal of thiol collectors by O_3 could be well described by the pseudo first-order kinetic models. By comparing rate constant of $k_{collector}$, it could be seen that the degradation by O_3, for the four collectors, followed the order of $k_{SN\text{-}9} > k_{EX} > k_{Z\text{-}200} > k_{DDA}$. Especially, the $k_{collector}$ of SN-9 and EX was almost three times higher than that of Z-200 and DDA. The results revealed that in terms of ozonation, the SN-9 and EX could be easily decomposed, but the Z-200 and DDA were refractory flotation reagents.

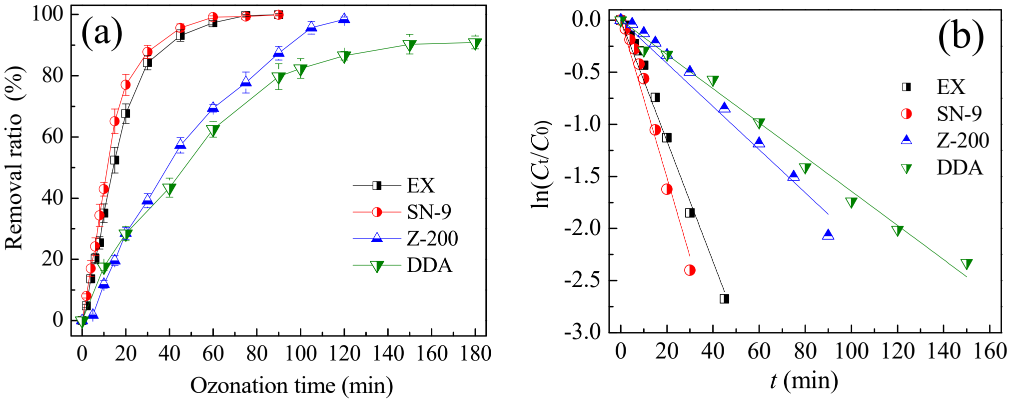

Figure 3. The variations of the removal ratio of thiol collectors with ozonation time (**a**) and the pseudo-first-order kinetic fitting of $\ln(C_t/C_0)$ *versus* ozonation time t (**b**).

Table 2. Kinetic equations, pseudo-first-order rate constants ($k_{collector}$), half-life time ($t_{1/2}$) and correlation coefficients (R^2) in the ozonation of thiol collectors.

Collector	Kinetic Equation	$k_{collector}$ (min^{-1})	$t_{1/2}$ (min)	R^2
EX	$C_t = C_0 \cdot e^{-0.0579t}$	0.0579	11.97	0.9903
SN-9	$C_t = C_0 \cdot e^{-0.0687t}$	0.0687	10.09	0.9918
Z-200	$C_t = C_0 \cdot e^{-0.0194t}$	0.0194	35.69	0.9835
DDA	$C_t = C_0 \cdot e^{-0.0164t}$	0.0164	42.27	0.9967

Due to low operation cost, the biodegradation has been tested to degrade some flotation reagents. The first-order biodegradation rate constants of SN-9 and Z-200 were reported to be 3.13×10^{-4} and 4.17×10^{-5} min^{-1}, respectively [13]. By comparing the $k_{SN\text{-}9}$ (0.0687 min^{-1}) and $k_{Z\text{-}200}$ (0.0194 min^{-1}) in Table 2, it was clear that the rate constant in ozonation was two-three orders higher than that in the biodegradation of same flotation reagent. The ozonation even at a low O_3 dosage achieved a much higher efficiency than the biodegradation in degrading flotation reagents.

Nowadays, residual flotation reagents are usually removed in tailing ponds with a natural degradation process. The first-order rate constant of EX natural degradation has been reported by Sun et al. [4] to be 2.094×10^{-5} min^{-1}, with a half-life of 22.99 day, at pH 7 and 25 °C, and have been given by Shen et al. [30] to be 1.55×10^{-5} min^{-1}, at pH 6.8 and 20 °C. Chen et al. [31] observed almost no natural degradation of EX at a pH ≥ 5, in 4 h. However, for the EX degradation, the ozonation at a low O_3 dosage of 1.125 mg/(min·L) could achieve the k_{EX} of 0.0579 min^{-1}, with a half-life of 11.97 min. Therefore, compared to a natural degradation process, ozonation at low O_3 dosage can effectively degrade flotation reagents, within a much shorter treatment time.

3.2. Carbon and Sulfur Mineralization of Thiol Collectors

In the ozonation of the thiol collectors, the concentrations of COD, TOC, and SO_4^{2-} ions were measured, as illustrated in Figure 4. For all collectors investigated, the concentration of both COD and TOC decreased with the increase of SO_4^{2-} concentration while the collector was degraded. Compared to the significant decrease of COD, the decline of TOC was much slower. As shown in Table 3, at the collector removal ratio of >90%, the removal ratio of COD was approximately below 62% and the carbon mineralization ratio (γ_C) was just lower than 27%, respectively. When comparing the rate constants of collector and COD removal (summarized in Tables 2 and 3), the $k_{\text{collector}}$ value was found to be 2–10 times higher than the k_{COD}, for each collector. It was revealed that only a small fraction of carbon in thiol collectors was completely mineralized by O_3, although all of the above 90% of collectors were decomposed. In the ozonation of *n*-butyl xanthate, *n*-butanol was detected by UPLC/Q-TOF-MS [32], and *O*-butyl peroxydithiocarbonate was found [11]. Thus, it could be reasonably inferred that most organic carbon in thiol collectors were still in the forms of reductive organic intermediates, after the ozonation.

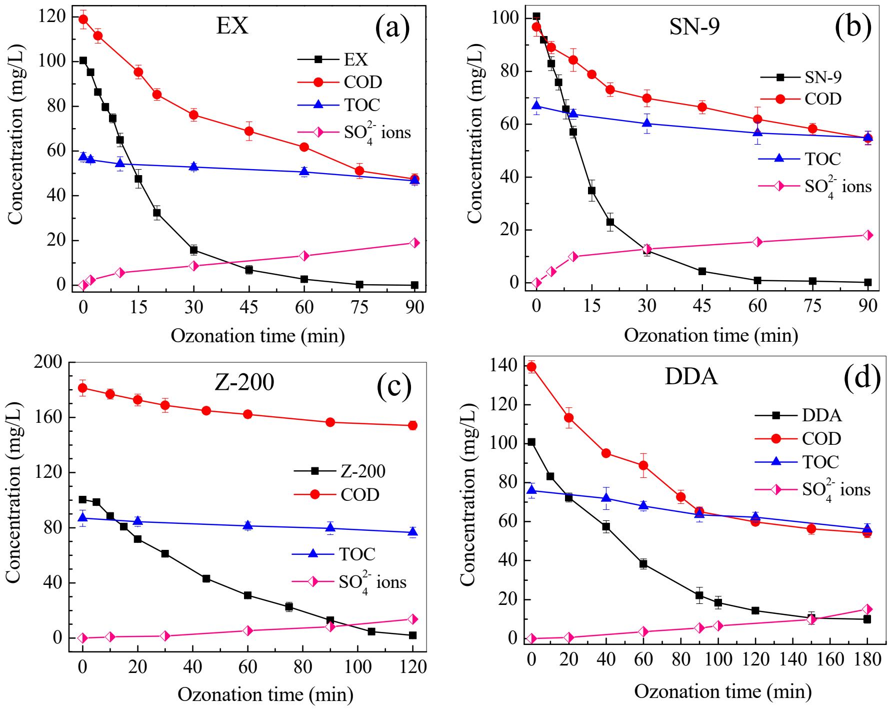

Figure 4. The variations of the concentration of collector, COD, TOC, and SO_4^{2-} ions with ozonation time in the degradation of EX (**a**), SN-9 (**b**), Z-200 (**c**), and DDA (**d**).

As illustrated in Figure 4, the concentration of SO_4^{2-} ions increased to 18.93 mg/L for EX, 18.07 mg/L for SN-9, 13.65 mg/L for Z-200, and 15.01 mg/L for DDA, respectively, at the end of ozonation. The generation of the $SO_4{}^{2-}$ ions indicated the complete oxidation of organic sulfur in the thiol collectors. However, as given in Table 3, the sulfur mineralization ratio (γ_S) was just below 22%, indicating that some sulfur byproducts, such as CS_2, S^{2-} and organics containing sulfur, might exist in solutions [10,11,30,32]. As volatile sulfur species such as CS_2 and H_2S were generated, they may have been emitted from ozone-bubbled solutions into a gas phase, resulting in lower γ_S values. For example, Yan et al. [32] had inferred the emitting of 20.6% sulfur into the gas phase in decomposing *n*-butyl xanthate by O_3. Generally, in this work, the mineralization ratio of carbon and sulfur for the four collectors ranged from 10% to 27%, at the collector removal ratio of above 90%.

Table 3. The removal ratio of the collector and the COD, the carbon and sulfur mineralization ratio, and the pseudo-first-order rate constants for COD removal, in the ozonation of thiol collectors.

Collector	Removal Ratio of Collector (%)	Removal of COD			Mineralization Ratio (%)	
		Removal Ratio of COD (%)	k_{COD} (min^{-1})	R^2	Carbon	Sulfur
EX	99.98 (90 min)	60.04 (90 min)	0.0111	0.9843	18.42 (90 min)	11.95 (90 min)
SN-9	99.87 (90 min)	43.47 (90 min)	0.00694	0.9838	17.84 (90 min)	21.21 (90 min)
Z-200	87.38 (90 min) 98.37(120 min)	13.67 (90 min) 14.97 (120 min)	0.00188	0.9858	8.31 (90 min) 11.82 (120 min)	12.54 (90 min) 20.92 (120 min)
DDA	79.71 (90 min) 90.91(180 min)	53.25 (90 min) 61.11 (180 min)	0.00779	0.9888	16.35 (90 min) 26.05 (180 min)	7.89 (90 min) 21.98 (180 min)

As given in Table 3, the γ_C of Z-200 at 90 min was just 8.31%, much lower than that of EX, SN-9, and DDA at 90 min. The k_{COD} of EX, SN-9, and DDA was 5.91, 3.69, and was 4.14 folds higher than that of Z-200, respectively. It clearly revealed that the intermediates derived from the Z-200 were hardly oxidized by O_3. Although the DDA was very refractory in the ozonation, the γ_C of the DDA was close to that of EX and SN-9 at 90 min, indicating that its intermediates could be readily decomposed by O_3. By considering γ_C and γ_S together, the mineralization of four collectors by O_3 had the following order: SN-9 $\approx$ EX > DDA > Z-200.

In general, ozonation reactions are divided into two main pathways—direct ozone oxidation, occurring at pH < 4.0 and indirect ozone oxidation, occurring at pH > 10.0. At the pH of 4.0–10.0, both pathways exist, but direct ozone oxidation becomes predominant in the neutral and weak acid medium [33,34]. As shown in Figure 5, the solution pH decreased from 10.0, initially, to 8.0–9.0 at the end of ozonation. Therefore, in this case, the direct ozone oxidation might have greatly contributed to the collector decomposition during most of the ozonation period. Unfortunately, the direct oxidation of organics by O_3 has some disadvantages of low reaction rate and strong selectivity, as compared to oxidation by free radicals [35–37]. Thus, the intermediates, hardly oxidized by O_3 molecules, should be accumulated in the solutions.

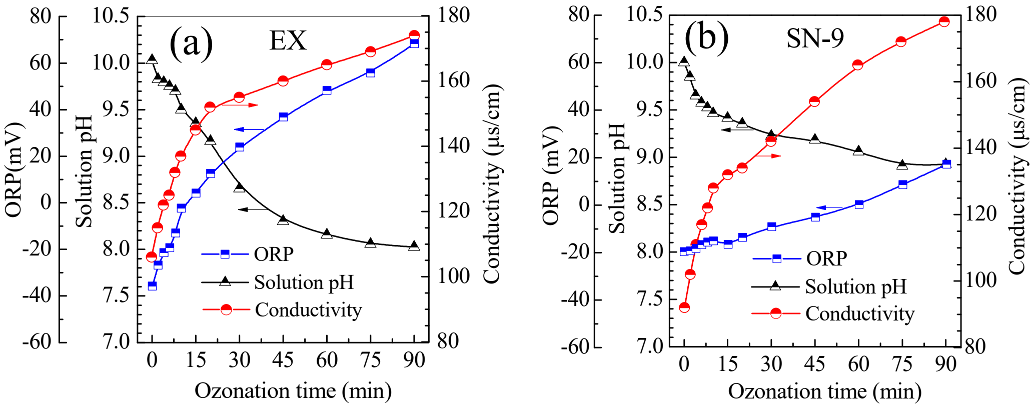

Figure 5. *Cont.*

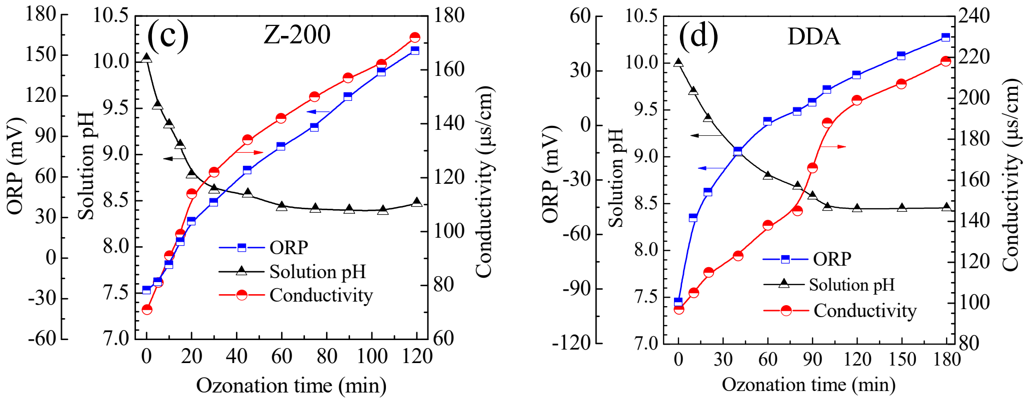

Figure 5. The variations of solution pH, conductivity, and ORP, with ozonation times, in the degradation of EX (**a**), SN-9 (**b**), Z-200 (**c**), and DDA (**d**).

3.3. Variation of Biodegradability

Although biodegradation is a low-cost procedure for removing organic pollutants, some flotation reagents, such as *n*-butyl xanthate [10], butyl amine aerofloat [10], ethylthionocarbamate [13], turpentine [38], isopropyl xanthate [39], and aniline aerofloat [40], are hardly biodegraded due to their special molecular structures. However, the intermediates derived by O_3, from these reagents, might become biodegradable [10]. Thus, a combined ozonation and biodegradation process may be more feasible than ozonation or biodegradation alone, in treating flotation effluents.

In this study, the variation of biodegradability of thiol collectors, before and after ozonation, was investigated. As shown in Figure 6, the BOD_5/COD for EX, SN-9, Z-200, and DDA solutions before the ozonation was 0.33, 0.19, 0.088, and 0.12, respectively. In general, organic pollutants with the BOD_5/COD of >0.3 are considered to be biodegradable [10]. Thus, it was clear that excepting the EX, the SN-9, Z-200, and DDA were biologically persistent flotation reagents. After ozonation for 90 min, the BOD_5/COD for EX, SN-9, and DDA solutions increased to 0.73, 0.31, and 0.32, respectively, indicating the generation of biodegradable intermediates. However, the BOD_5/COD for Z-200 solution just increased from 0.088 to 0.15, after ozonation for 120 min, revealing that its intermediates were still hardly biodegraded. It can be seen that both the Z-200 and its intermediates were biologically persistent organics. For all four collectors investigated, the increase of the biodegradability, after the ozonation, followed the order of EX > DDA ≈ SN-9 > Z-200.

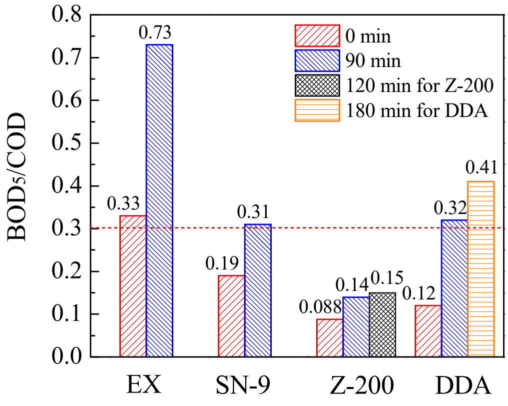

Figure 6. The biodegradability of collector solutions before and after the ozonation, for different treatment times.

3.4. Evolution of Solution pH, ORP and Conductivity

In the flotation of sulfide minerals, solution parameters such as pulp pH and ORP are very important in determining the floatability of minerals and interaction of flotation reagents with minerals [41–44]. Since treated flotation effluents will be reused in flotation circuits as feeding water, the changes of both solution parameters and reagent concentrations should be revealed to better understand the quality of reused flotation water. However, in the previous works of degrading flotation reagents by O_3 [10,11,32], H_2O_2 [31], Fenton reagents [45], and sodium hypochlorite [9], little attention was paid to revealing the evolution of solution parameters, except for the pH value.

In this work, the solution pH, ORP, and conductivity in degrading collectors were recorded as shown in Figure 5. For four collectors studied, the solution pH was declined from 10.0 to 8.0–9.0, and the increase of the conductivity reached 68, 86, 101, and 121 µs/cm for EX, SN-9, Z-200, and DDA solution, respectively, at the collector removal ratio of >90%. The indirect ozonation reactions were initiated with catalytic decomposition of O_3 by OH^- ions, as shown in Equations (6)-(11) [23,24]. The chain reactions of O_3 decomposition could generate free radicals, such as OH, HO_2, and$\cdot O_2{}^-$, which were responsible for breaking the chemical bonds of organics. Thus H^+ ions were continually dissociated from H_2O, with an observed decrease of solution pH. In addition, simple carboxylic acids, such as formic and acetic acids could be generated via indirect reactions [46,47], which also contributed to the acidity of collector solutions. Thus, the pH of collector solutions was decreased after the ozonation.

$$H_2O \leftrightarrow H^+ + OH^- \tag{6}$$

$$O_3 + OH^- \rightarrow HO_2 + O_2^- \tag{7}$$

$$HO_2 \rightarrow H^+ + O_2^- \tag{8}$$

$$O_3 + O_2^- \rightarrow O_3^- + O_2 \tag{9}$$

$$O_3^- + H^+ \rightarrow HO_3 \tag{10}$$

$$HO_3 \rightarrow OH + O_2 \tag{11}$$

In the degradation of xanthates by O_3 or H_2O_2, inorganic ions, such as S^{2-}, $S_2O_3{}^{2-}$, $SO_4{}^{2-}$ and $CO_3{}^{2-}$ were observed to be readily generated [10,11,31]. Ionized intermediates, such as *O*-ethyl thiocarbonate (ETC^-) and *O*-ethyl peroxydithiocarbonate (EPX^-) were also detected in the oxidation of EX by H_2O_2 [17]. Therefore, the increase of conductivity directly revealed that some ionic intermediates were generated in the ozonation of collectors. The higher conductivity in Figure 5 corresponded to a lower concentration of collector and COD, as shown in Figure 4.

In the ozonation process, it is frequently observed that the ozone consumption rate will remarkably decrease with a rapid increase of the ORP and the reduction of pollutant removal efficiency, while the pollutant concentration goes below a certain value [48,49]. So, the ORP is a useful indicator in the control of O_3 addition, to minimize the process cost [48,50,51]. For the mineral flotation, the ORP is found to determine the oxidation of collectors and speciation of metal ions [41,44]. Thus, the revelation of ORP evolution is very important for both the control of O_3 addition and the reuse of treated flotation effluents.

As shown in Figure 5, the ORP of collector solutions, before ozonation, was negative. As the ozonation reactions occurred, the ORP increased up to 68.3, 17.2, 150.3, and 48.4 mV for EX, SN-9, Z-200, and DDA solutions, at the end of ozonation, respectively. The variations of COD concentration with the ORP are shown in Figure 7. The ORP of ozonated solutions increased with the reduction of the COD for the four collectors. Thus, it can be inferred that a certain correlation should exist between the COD and ORP of ozonated solutions, which might allow the ORP, as the indicator, to control the ozonation process.

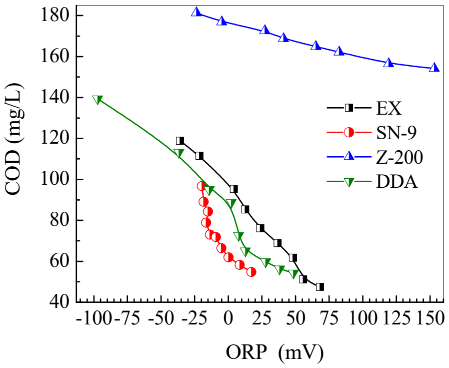

Figure 7. The variations of COD concentration with the ORP of ozonated collector solutions.

3.5. Ozone Utilization

At the O_3 dosage of 1.125 mg/(min·L), the O_3 input rate was 2.26 mg/min. As shown in Figure 8, the O_3 emitting rate for deionized water at pH 10.0 was just 0.495 mg/min, and the O_3 utilization ratio (η_{O3}) of 78.01% was achieved. The color of KI absorption liquid was changed from a dark red, due to the absorption of the input O_3 gas, to a light yellow for the absorption of the O_3 emitted from water. The result revealed that 78.01% of input O_3 was dissolved and decomposed in alkaline water. Since OH^- ions could catalytically decompose dissolved O_3 as given in Equations (6)–(11), the alkalinity of water promoted the dissolution of gaseous O_3 into water, resulting in a lower O_3 emitting rate. It suggests that the alkalinity of flotation effluents is beneficial to the O_3 utilization and generation of free radicals (OH, $\cdot HO_2$ and $O_2{}^-$, etc.). In this work, low O_3 dosage should have also contributed to a high η_{O3}, for deionized water.

When the collector concentration was raised from 1 to 100 mg/L, the η_{O3} shown in Figure 8b increased from 94.22% to 99.89%, for thee EX and from 88.62% to 99.97%, for the DDA solution, respectively. The color of the KI absorption liquids, for absorbing the O_3 emitted, from the 100 mg/L EX and DDA solutions was almost white, directly demonstrating nearly no escape of O_3 from the reactors. It was very clear that the addition of collectors increased the O_3 utilization, which could be attributed to the reactions of O_3 molecules, with collectors. As shown in Figure 8b, the EX had higher η_{O3} than the DDA, while the concentration was <10 mg/L. The difference in η_{O3} directly revealed that the EX was more sensitive in reacting with O_3 than the DDA. In this work, at a low O_3 dosage of 1.125 mg/(min·L), the η_{O3} was close to 100%, in the ozonation of EX and DDA with 100 mg/L concentration. However, in the ozonation of *n*-butyl xanthate, the achieved η_{O3} just ranged from 7.2% to 51.7%, at the O_3 dosage of 5.88-50.36 mg/(min·L) [11]. The results revealed that the ozonation of thiol collectors at a low O_3 dosage could achieve almost 100% utilization of O_3, meaning it reduced the treating cost by adding a lesser amount of O_3.

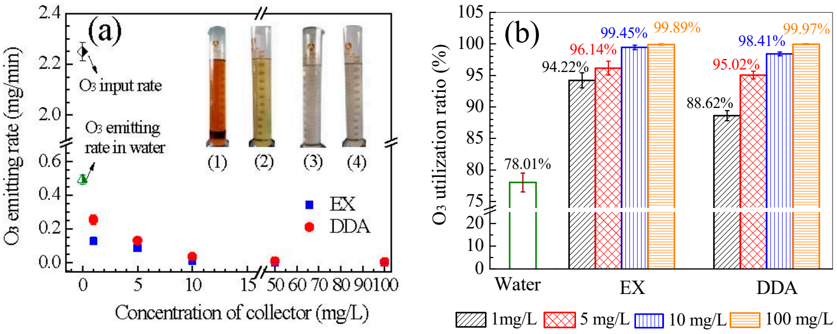

Figure 8. Ozone-emitting rate (**a**) and O_3 utilization ratio (**b**) in the ozonation of EX and DDA, with different concentrations. The inset figures are photographs of KI absorption liquids, for absorbing input O_3 gas (1), emitted O_3 from deionized water (2), EX (3), and DDA (4) solutions with 100 mg/L concentration, respectively.

3.6. Analysis of Energy Consumption Efficiency

In the treatment of contaminants with AOPs, the electrical energy per order (*EE/O*) was introduced to directly evaluate the electric efficiency and feasibility of the scale-up of AOPs [52]. This parameter was defined as "the electric energy in kWh required in degrading a contaminant by one order of magnitude in 1 m^3 contaminated water". To calculate the energy requirements for the ozonation, an average energy consumption of 15 kWh/kg for the O_3 production was assumed [53], and the energy calculations were based on a 90% removal of collectors. *EE/O* values (kWh/(m^3·order)) were calculated for batch operations as given by Equation (12).

$$EE/O = \frac{P \times 1000}{V \times 60} \times \frac{\ln 10}{k_{\text{collector}}} \tag{12}$$

where P was the electric power (kWh) required for producing dosed O_3, V was the volume (L) of test collector solution, and $k_{\text{collector}}$ was the pseudo-first-order constant (min^{-1}).

The results of the energy calculation for the ozonation of the four collectors are summarized in Table 4. As shown in Table 2, the $k_{\text{collector}}$ of EX and SN-9 was lower than that of Z-200 and DDA, revealing the higher efficiency in the degradation of EX and SN-9. Thus, the *EE/O* values for EX and SN-9 removal were much lower than that for Z-200 and DDA. However, at a low O_3 dosage of 1.125 mg/(min·L), the ozonation of all of four collectors was feasible, in terms of energy consumption, since values of *EE/O*, not higher than 10 kWh/(m^3·order), were considered suitable for practical application [54].

Table 4. Electrical energy per order (*EE/O*) in the ozonation of the four thiol collectors.

Collector	EX	SN-9	Z-200	DDA
EE/O (kWh/(m^3·order))	0.45	0.33	3.18	6.06

4. Conclusions

Thiol collectors (EX, SN-9, Z-200 and DDA) could be effectively degraded by O_3 at a low dosage of 1.125 mg/(min·L). Both the removal of collectors and the decline of COD followed the pseudo-first-order kinetic models. The ozonation of the four collectors followed the order of $k_{\text{collector}}$: $k_{\text{SN-9}}$ (0.0687 min^{-1}) > k_{EX} (0.0579 min^{-1}) > $k_{\text{Z-200}}$ (0.0194 min^{-1}) > k_{DDA} (0.0164 min^{-1}). The $k_{\text{collector}}$ in the removing-collectors was 2-10 times higher than the k_{COD} of COD removal. At the collector removal ratio of >90%, the mineralization ratio of the four collectors ranged from 10% to 27%, with the order of SN-9 ≈ EX > DDA > Z-200. For the four collectors investigated, EX and SN-9 could be easily degraded by O_3, but the ozonation of Z-200 and DDA exhibited much lower efficiencies. Especially, both the Z-200 and its intermediates were hardly decomposed by O_3.

The SN-9, Z-200, and DDA were found to be biologically persistent flotation reagents as their BOD_5/COD values were below 0.2. After ozonation, the BOD_5/COD of EX, SN-9, and DDA solutions increased to 0.73, 0.31, and 0.41, respectively, with remarkable increase of the biodegradability. However, the BOD_5/COD of Z-200 solution increased just from 0.088 to 0.15, after the ozonation, revealing that its intermediates were still hardly biodegraded. After ozonation, the solution pH of four collectors decreased from 10.0 to 8.0–9.0, and an increase of conductivity (68–121 μs/cm) was observed, exhibiting the generation of various ionic intermediates. For the four collectors, the ORP rapidly increased with the decline of COD concentration, indicating that the ORP might act as the indicator to monitor the ozonation of collectors.

At low O_3 dosage of 1.125 mg/(min·L), the η_{O3} reached 78.01% for ionized water at pH 10.0 due to effective O_3 decomposition initiated by OH^- ions. The addition of collectors significantly enhanced the O_3 decomposition. At the collector (EX and DDA) concentration of >10 mg/L, the η_{O3} increased to above 98.41%, revealing an almost complete usage of input O_3 at a low O_3 dosage. *EE/O* values revealed that the ozonation of all of four collectors was feasible, in terms of energy consumption.

Author Contributions: P.F. and H.P. designed the study. G.L. and Z.C. set up the experimental degradation systems. X.L., G.L. and H.P. performed the degradation experiments of four collector solutions and analyzed the water quality parameters (pH, ORP and conductivity) and the concentration of collector, COD and SO_4^{2-} ions. X.L. and Z.C. carried out the analysis of TOC and ozone concentration in gas phase. All of the authors interpreted experimental results and supported the preparation of the paper. P.F. had revised the manuscript.

Funding: This research was funded by the National Natural Science Foundation of China, grant number 51674017.

Acknowledgments: We were grateful to Center for Environmental Quality Test, Tsinghua University for providing the analysis of BOD_5 concentration of collector solution samples.

Conflicts of Interest: The authors declare no conflict of interest.

References

1. Bulatovic, S.M. *Handbook of Flotation Reagents: Chemistry, Theory and Practice*, 1st ed.; Elsevier: Amsterdam, The Netherlands, 2010.
2. Somasundaran, P.; Moudgil, B.M. *Reagents in Mineral Technology*; Marcel Dekker Inc.: New York, NY, USA, 1988.
3. Li, X.F. Teratogenic toxicity of butyl xanthate to frog embryos. *Environ. Sci. Acta* **1990**, *10*, 213–216.
4. Sun, Z.X.; Forsling, W. The degradation kinetics of ethyl xanthate as a function of pH in aqueous solution. *Miner. Eng.* **1997**, *10*, 389–400. [CrossRef]
5. Kemppinen, J.; Aaltonen, A.; Sihvonen, T.; Leppinen, J.; Sirén, H. Xanthate degradation occurring in flotation process waters of a gold concentrator plant. *Miner. Eng.* **2015**, *80*, 1–7. [CrossRef]
6. Rao, S.R.; Finch, J.A. A review of water reuse in flotation. *Miner. Eng.* **1989**, *2*, 65–85. [CrossRef]
7. Mielczarski, J. The role of impurities of sphalerite in the adsorption of ethyl xanthate and its flotation. *Int. J. Miner. Process.* **1986**, *16*, 179–194. [CrossRef]
8. Rezaei, R.; Massinaei, M.; Zeraatkar Moghaddam, A. Removal of the residual xanthate from flotation plant tailings using modified bentonite. *Miner. Eng.* **2018**, *119*, 1–10. [CrossRef]
9. Lin, W.X.; Tian, J.; Ren, J.; Xu, P.T.; Dai, Y.K.; Sun, S.Y.; Wu, C. Oxidation of aniline aerofloat in flotation wastewater by sodium hypochlorite solution. *Environ. Sci. Pollut. Res.* **2016**, *23*, 785–792. [CrossRef] [PubMed]
10. Liu, R.Q.; Sun, W.; Ouyang, K.; Zhang, L.M.; Hu, Y.H. Decomposition of sodium butyl xanthate (SBX) in aqueous solution by means of OCF: Ozonator combined with flotator. *Miner. Eng.* **2015**, *70*, 222–227. [CrossRef]
11. Fu, P.F.; Feng, J.; Yang, T.W.; Yang, H.F. Comparison of alky xanthates degradation in aqueous solution by the O_3 and UV/O_3 process: Efficiency, mineralization and ozone utilization. *Miner. Eng.* **2015**, *81*, 128–134. [CrossRef]
12. Fu, P.F.; Feng, J.; Yang, H.F.; Yang, T.W. Degradation of *n*-butyl xanthate by vacuum UV-ozone (VUV/O_3) in comparison with ozone and VUV photolysis. *Process Saf. Environ. Prot.* **2016**, *102*, 64–70. [CrossRef]
13. Chen, S.H.; Gong, W.Q.; Mei, G.J.; Zhou, Q.; Bai, C.P.; Xu, N. Primary biodegradation of sulfide mineral flotation collectors. *Miner. Eng.* **2011**, *24*, 953–955. [CrossRef]
14. Araujo, D.M.; Yoshida, M.I.; Takahashi, J.A.; Carvalho, C.F.; Stapelfeldt, F. Biodegradation studies on fatty amines used for reverse flotation of iron ore. *Int. Biodeterior. Biodegrad.* **2010**, *64*, 151–155. [CrossRef]
15. Jafari, M.; Shafaei, S.Z.A.; Abdollahi, H.; Gharabaghi, M.; Chelgani, S.C. A comparative study on the effect of flotation reagents on growth and iron oxidation activities of *Leptospirillum ferrooxidans* and *Acidithiobacillus ferrooxidans*. *Minerals* **2017**, *7*, 2. [CrossRef]
16. Mahiroglu, A.; Tarlan-Yel, E.; Sevimli, M.F. Treatment of combined acid mine drainage (AMD)-flotation circuit effluents from copper mine via Fenton's process. *J. Hazard. Mater.* **2009**, *166*, 782–787. [CrossRef] [PubMed]
17. Silvester, E.; Truccolo, D.; Hao, F.P. Kinetics and mechanism of the oxidation of ethyl xanthate and ethyl thiocarbonate by hydrogen peroxide. *J. Chem. Soc. Perkin Trans.* **2002**, *2*, 1562–1571. [CrossRef]
18. Chen, S.H.; Xiong, P.; Zhan, W.; Xiong, L. Degradation of ethylthionocarbamate by pyrite-activated persulfate. *Miner. Eng.* **2018**, *12*, 38–43. [CrossRef]
19. Xiao, Q.; Ouyang, L.L. Photocatalytic photodegradation of xanthate over $Zn_{1\text{-}x}Mn_xO$ under visible light irradiation. *J. Alloys Compd.* **2009**, *479*, L4–L7. [CrossRef]
20. Molina, G.C.; Cayo, C.H.; Rodrigues, M.A.S.; Bernardes, A.M. Sodium isopropyl xanthate degradation by advanced oxidation processes. *Miner. Eng.* **2013**, *45*, 88–93. [CrossRef]

21. Feng, Q.C.; Wen, S.M.; Zhao, W.J.; Liu, J.; Liu, D. Effect of pH on surface characteristics and flotation of sulfidized cerussite. *Physicochem. Probl. Miner. Process.* **2016**, *52*, 676–689. [CrossRef]
22. Gibson, C.E.; Kelebek, S. Sensitivity of pentlandite flotation in complex sulfide ores towards pH control by lime versus soda ash: Effect on ore type. *Int. J. Miner. Process.* **2014**, *127*, 44–51. [CrossRef]
23. Staehelin, J.; Hoigné, J. Decomposition of ozone in water: Rate of initiation by hydroxide ions and hydrogen peroxide. *Environ. Sci. Technol.* **1982**, *16*, 676–681. [CrossRef]
24. Yershov, B.G.; Morozov, P.A.; Gordeev, A.V.; Seliverstov, A.F. Kinetic regularities of ozone decomposition in water. *J. Water Chem. Technol.* **2009**, *31*, 381–388. [CrossRef]
25. Wu, C.H.; Ng, H.Y. Degradation of C.I. Reactive Red 2 (RR2) using ozone-based systems: Comparisons of decolorization efficiency and power consumption. *J. Hazard. Mater.* **2008**, *152*, 120–127. [CrossRef] [PubMed]
26. Katsoyiannis, I.A.; Canonica, S.; von Gunten, U. Efficiency and energy requirements for the transformation of organic micropollutants by ozone, O_3/H_2O_2 and UV/H_2O_2. *Water Res.* **2011**, *45*, 3811–3822. [CrossRef] [PubMed]
27. Rahman, R.M.; Ata, S.; Jameson, G.J. Study of froth behaviour in a controlled plant environment-Part 2: Effect of collector and frother concentration. *Miner. Eng.* **2015**, *81*, 161–166. [CrossRef]
28. Wen, S.H.; Chen, L.; Li, W.Q.; Ren, H.Q.; Li, K.; Wu, B.; Hu, H.D.; Xu, K. Insight into the characteristics, removal, and toxicity of effluent organic matter from a pharmaceutical wastewater treatment plant during catalytic ozonation. *Sci. Rep.* **2018**, *8*, 9581. [CrossRef] [PubMed]
29. Ding, P.Y.; Chu, L.B.; Wang, J.L. Advanced treatment of petrochemical wastewater by combined ozonation and biological aerated filter. *Environ. Sci. Pollut. Res.* **2018**, *25*, 9673–9682. [CrossRef] [PubMed]
30. Shen, Y.; Nagaraj, D.R.; Farinato, R.; Somasundaran, P. Study of xanthate decomposition in aqueous solutions. *Miner. Eng.* **2016**, *93*, 10–15. [CrossRef]
31. Chen, X.H.; Hu, Y.H.; Peng, H.; Cao, X.F. Degradation of ethyl xanthate in flotation residues by hydrogen peroxide. *J. Cent. South Univ.* **2015**, *22*, 495–501. [CrossRef]
32. Yan, P.F.; Chen, G.Q.; Ye, M.Y.; Sun, S.Y.; Ma, H.T.; Lin, W.X. Oxidation of potassium n-butyl xanthate with ozone: Products and pathways. *J. Clean. Prod.* **2016**, *139*, 287–294. [CrossRef]
33. Beltran-Heredia, J.; Torregrosa, J.; Dominguez, J.R.; Peres, J.A. Kinetics of the reaction between ozone and phenolic acids present in agro-industrial wastewaters. *Water Res.* **2001**, *35*, 1077–1082. [CrossRef]
34. Beltran, F.J.; Garcia-Araya, J.F.; Alvarez, P.M. pH sequential ozonation of domestic and wine-distillery wastewaters. *Water Res.* **2001**, *35*, 929–936. [CrossRef]
35. Tobiasn, N.; Hans, F.; Clemens, V.S. Ozonation of wastewater: Rate of ozone consumption and hydroxyl radical yield. *Environ. Sci. Technol.* **2009**, *15*, 5990–5995. [CrossRef]
36. Hoigné, J.; Bader, H. Rate constants of reactions of ozone with organic and inorganic compounds in water-I Non-dissociating organic compounds. *Water Res.* **1983**, *17*, 173–183. [CrossRef]
37. Hoigné, J.; Bader, H. Rate constants of reactions of ozone with organic and inorganic compounds in water-II Dissociating organic compounds. *Water Res.* **1983**, *17*, 185–194. [CrossRef]
38. Cheng, H.; Lin, H.; Huo, H.X.; Dong, Y.B.; Xue, Q.Y.; Cao, L.X. Continuous removal of ore floatation reagents by an anaerobic–aerobic biological filter. *Bioresour. Technol.* **2012**, *114*, 255–261. [CrossRef] [PubMed]
39. Natarajan, K.A.; Sabari Prakasan, M.R. Biodegradation of sodium isopropyl xanthate by Paenibacillus polymyxa and Pseudomonas putida. *Miner. Metall. Process.* **2013**, *30*, 226–232. [CrossRef]
40. Song, W.F.; Chen, X.Q.; Yan, M.; Tang, T.Z.; Li, S.Y. Processing of aniline aerofloat wastewater with SBR system and its biodegradation mechanism. *Agric. Sci. Technol.* **2013**, *14*, 1032–1036.
41. López Valdivieso, A.; Sánchez López, A.A.; Ojeda Escamilla, C.; Fuerstenau, M.C. Flotation and depression control of arsenopyrite through pH and pulp redox potential using xanthate as the collector. *Int. J. Miner. Process.* **2006**, *81*, 27–34. [CrossRef]
42. Eliseev, N.I. Dixanthogen Formation in Flotation. *J. Min. Sci.* **2012**, *48*, 1065–1070. [CrossRef]
43. Montalti, M.; Fornasiero, D.; Ralston, J. Ultraviolet-visible spectroscopic study of the kinetics of adsorption of ethyl xanthate on pyrite. *J. Colloid Interface Sci.* **1991**, *143*, 440–450. [CrossRef]
44. Nava-Alonso, F.; Pecina-Treviño, T.; Pérez-Garibay, R.; Uribe-Salas, A. Pulp potential control in flotation: The effect of hydrogen peroxide addition on the extent of xanthate oxidation. *Can. Metall. Q.* **2002**, *41*, 391–397. [CrossRef]
45. Wang, X.Y.; Liu, W.G.; Duan, H.; Liu, W.B. Degradation mechanism study of amine collectors in Fenton process by quantitative structure-activity relationship analysis. *Physicochem. Probl. Miner. Process.* **2018**, *54*, 713–721. [CrossRef]

46. Hammes, F.; Salhi, E.; Koester, O.; Kaiser, H.P.; Egli, T.; von Gunten, U. Mechanistic and kinetic evaluation of organic disinfection by-product and assimilable organic carbon (AOC) formation during the ozonation of drinking water. *Water Res.* **2006**, *40*, 2275–2286. [CrossRef] [PubMed]
47. Ramseier, M.K.; von Gunten, U. Mechanisms of phenol ozonation-kinetics of formation of primary and secondary reaction products. *Ozone Sci. Eng.* **2009**, *31*, 201–215. [CrossRef]
48. Wu, T.T.; Englehardt, J.D. Peroxone mineralization of chemical oxygen demand for direct potable water reuse: Kinetics and process control. *Water Res.* **2015**, *73*, 362–372. [CrossRef] [PubMed]
49. Chiang, Y.P.; Liang, Y.Y.; Chang, C.N.; Chao, A.C. Differentiating ozone direct and indirect reactions on decomposition of humic substances. *Chemosphere* **2006**, *65*, 2395–2400. [CrossRef] [PubMed]
50. Contreras, E.M.; Bertola, N.C.; Zaritzky, N.E. Monitoring the ozonation of phenol solutions at constant pH by different methods. *Ind. Eng. Chem. Res.* **2011**, *50*, 9799–9809. [CrossRef]
51. Lan, B.Y.; Nigmatullin, R.; Puma, G.L. Ozonation kinetics of cork-processing water in a bubble column reactor. *Water Res.* **2008**, *42*, 2473–2482. [CrossRef] [PubMed]
52. Bolton, J.R.; Bircger, K.G.; Tumas, W.; Tolman, C.A. Figure-of-merit for the technical development and application of advanced oxidation technologies for both electric- and solar-derived systems. *Pure Appl. Chem.* **2001**, *73*, 627–637. [CrossRef]
53. Rosenfeldt, E.J.; Linden, K.G.; Canonica, S.; von Gunten, U. Comparison of the efficiency of OH radical formation during ozonation and the advanced oxidation processes O_3/H_2O_2 and UV/H_2O_2. *Water Res.* **2006**, *40*, 3695–3704. [CrossRef] [PubMed]
54. Goslan, E.H.; Gurses, F.; Banks, J.; Parsons, S.A. An investigation into reservoir NOM reduction by UV photolysis and advanced oxidation processes. *Chemosphere* **2006**, *65*, 1113–1119. [CrossRef] [PubMed]